Limiting Fragmentation in Oxygen-Induced Emulsion Interactions at 14.6, 60, and 200 GeV/nucleon

M. I. Adamovich,[10] M. M. Aggarwal,[3] R. Arora,[3] Y. A. Alexandrov,[10] S. A. Azimov,[14] E. Basova,[13] K. B. Bhalla,[5] A. Bhasin,[6] V. S. Bhatia,[3] R. A. Bondarenko,[13] T. H. Burnett,[12] X. Cai,[15] L. P. Chernova,[14] M. M. Chernyavski,[10] B. Dressel,[9] E. M. Friedlander,[2] S. I. Gadzhieva,[14] E. R. Ganssauge,[9] S. Garpman,[7] S. G. Gerassimov,[10] A. Gill,[5] J. Grote,[12] K. G. Gulamov,[14] U. G. Gulyamov,[13] S. Hackel,[9] H. H. Heckman,[2] B. Jakobsson,[7] B. Judek,[11] S. Kachroo,[6] F. G. Kadyrov,[14] H. Kallies,[9] L. Karlsson,[7] G. L. Kaul,[6] M. Kaur,[3] S. P. Kharlamov,[10] V. Kumar,[5] P. Lal,[5] V. G. Larionova,[10] P. J. Lindstrom,[2] L. S. Liu,[15] S. Lokanathan,[5] J. Lord,[12] N. S. Lukicheva,[14] L. K. Mangotra,[6] N. V. Maslennikova,[10] I. S. Mittra,[3] E. Monnand,[4] S. Mookerjee,[5] C. Mueller,[9] S. H. Nasyrov,[13] V. S. Navotny,[14] G. I. Orlova,[10] I. Otterlund,[7] N. G. Peresadko,[10] S. Persson,[7] N. V. Petrov,[13] W. Y. Qian,[15] R. Raniwala,[5] S. Raniwala,[5] N. K. Rao,[6] J. T. Rhee,[9] N. Saidkhanov,[13] N. A. Salmanova,[10] W. Schultz,[9] F. Schussler,[4] V. S. Shukla,[5] D. Skelding,[12] K. Söderström,[7] E. Stenlund,[7] R. S. Storey,[11] J. F. Sun,[8] L. N. Svechnikova,[14] M. I. Tretyakova,[10] T. P. Trofimova,[13] H. Q. Wang,[15] Z. O. Weng,[8] R. J. Wilkes,[12] G. F. Xu,[1] D. H. Zhang,[8] P. Y. Zheng,[1] D. C. Zhou,[15] and J. C. Zhou[15]

(EMU01 Collaboration)

[1]*Academica Sinica, Beijing, Peoples Republic of China*
[2]*Lawrence Berkeley Laboratory, University of California, Berkeley, California 94720*
[3]*Panjab University, Chandigarh, India*
[4]*Centre d'Etudes Nucléares, Grenoble, France*
[5]*University of Rajasthan, Jaipur, India*
[6]*University of Jammu, Jammu, India*
[7]*University of Lund, Lund, Sweden*
[8]*Shanxi Normal University, Linfen, Peoples Republic of China*
[9]*Philipps University, Marburg, West Germany*
[10]*Lebedev Institute, Moscow, U.S.S.R.*
[11]*National Research Council of Canada, Ottawa, Canada*
[12]*University of Washington, Seattle, Washington 98195*
[13]*Institute of Nuclear Physics, Tashkent, U.S.S.R.*
[14]*Physical-Technical Institute, Tashkent, U.S.S.R.*
[15]*Hua-Zhong Normal University, Wuhan, Peoples Republic of China*
(Received 15 December 1988)

Pseudorapidity distributions of relativistic singly charged particles in oxygen-induced emulsion interactions at 14.6, 60, and 200 GeV/nucleon are studied. Limiting fragmentation behavior is observed in both the target and projectile fragmentation regions for a central as well as for a minimum-bias sample. Comparisons with the FRITIOF model reveal that the picture of fragmenting strings successfully describes the observed data.

PACS numbers: 25.70.Np

The efforts at CERN (60 and 200 GeV/nucleon) and at BNL (14.6 GeV/nucleon) to accelerate heavy ions to ultrarelativistic energies in order to obtain the necessary requirements for the creation of a quark-gluon plasma state have resulted in a lot of experimental data on various projectile-target combinations.[1,2] The emulsion technique allows studies of produced charged particles and their distributions in space with higher accuracy and a larger acceptance than most of the current counter experiments, although with rather limited statistics. A great advantage with emulsions is that the same projectile-target system can be studied at the three available energies with identical detectors and with identical analysis criteria. In this Letter we will focus on pseudorapidity ($\eta = -\ln\tan\Theta/2$) distributions of charged particles emerging from interactions between oxygen and emulsion nuclei.

In the EMU01 experiments two complementary exposure techniques were used, each having its own advantages. The technique utilizing vertically exposed emulsion chambers has been described elsewhere.[2] In this Letter we report on results obtained using conventional emulsion stacks exposed horizontally. These stacks consist of 30 BR-2-type pellicles, each of size $20\times10\times0.06$

or $10\times10\times0.06$ cm^3. The sensitivity varies between 20 and 30 grains per 100 μm for minimum-ionizing particles. The density of the beam was about 5×10^3 nuclei/cm^2.

Interactions were found by along-the-track scanning, which is the optimal method for obtaining a minimum-bias sample. Each projectile was followed up to a distance of 6 to 7 cm from the point of incidence, and the minimum-bias samples were obtained from completely measured events found at a distance 2–5 cm from the front edge. At larger distances from the front edge measurements were prevented due to the background of secondary particles emerging from upstream interactions. Measurements of small-angle tracks ($\Theta\leq10°$ -15°) were done relative to noninteracting beam tracks selected in the vicinity, enabling an accuracy of about $\Delta\Theta=0.1$ mrad for angles $\Theta\leq1$ mrad. For each event the multiplicity of shower particles, n_s, and of target-associated particles, N_h, was determined. The shower particles are singly charged particles with $\beta>0.7$ and the target-associated particles are mainly knockout protons and evaporation fragments from the target. Projectile fragments with $Z\geq2$ were charge determined by the δ-electron or gap density counting methods. The spectator fragments with $Z=1$ were assumed to be among the shower particles having $\Theta\leq\Theta_c=0.2/p_{\text{beam}}$. All singly charged particles within this cone were excluded from the number n_s. The value of Θ_c has been chosen so that the probability of including produced particles among the fragments is minimized. Events produced by electromagnetic dissociation and elastic scattering were removed from the final samples by the requirement $n_s\geq1$. In all such events, all of the 8 projectile charges were found inside the cone.

Besides the three data samples, two samples consisting of $\simeq10000$ events from the Lund model FRITIOF (version 1.7)[3] were generated, one at 60A GeV and one at 200A GeV. The FRITIOF samples were subject to the same restrictions as the real data. The fraction of events from the different target nuclei in emulsion was simulated using known data on the chemical composition of the emulsion. No FRITIOF sample was produced for 14.6A GeV, since the foundations of the model prohibits its usage at too low energies. The fraction of events in the FRITIOF samples rejected due to the requirement $n_s\geq1$ is less than 0.5%, and gives an estimate of the systematic errors in the real data, introduced by this requirement. Table I summarizes some of the features of the different event samples.

TABLE I. Characteristics of the samples used.

	E_{inc}/A (GeV)	No. of events	σ_{inel}[a] (mb)	$\langle n_s\rangle$	Central sample (%)
Data	14.6	385	1050 ± 20	21.2 ± 1.1	7.5 ± 1.3
	60	372	1060 ± 40	40.6 ± 2.2	8.6 ± 1.5
	200	503	1090 ± 30	58.1 ± 2.8	10.1 ± 1.3
FRITIOF	60	9848	1000	39.4 ± 0.4	5.5 ± 0.2
	200	9788	1000	58.0 ± 0.6	7.9 ± 0.3

[a]Calculated as $\sigma=1/\rho\lambda$, where ρ is the atom density in nuclear emulsion, and λ is the observed mean free path measured for inelastic interactions.

In Figs. 1(a) and 1(b) the pseudorapidity distributions for the minimum-bias samples at the three different energies are compared. In Fig. 1(a) the comparison is made in the target rest frame and in 1(b) in the projectile rest frame. The projectile rest frame is obtained by using the approximation $\eta\simeq y=\frac{1}{2}\ln[(E+p_L)/(E-p_L)]$ and the well known boost invariance of rapidity. η_p is given by $\eta_p\simeq-\ln(\langle p_T^\pi\rangle m_p/2\langle m_T^\pi\rangle p_{\text{inc}})\simeq y_p+0.08$, where $\langle m_T^\pi\rangle$ is the average transverse mass of a pion with average transverse momentum $\langle p_T^\pi\rangle=0.34$ GeV/c. m_p is the proton mass and p_{inc} its incident momentum. η_p thus corresponds to the average pseudorapidity of a pion emerging from the projectile system. For the three energies η_p is 3.58, 4.95, and 6.14, respectively. In Fig. 1(a) we clearly see evidence for limiting fragmentation in the target fragmentation region, where the distributions from the three energies fall on top of each other below $\eta\simeq1$. We also see that for the two higher energies the distributions coincide up to $\eta\simeq2$, showing that the extension of the region of limiting fragmentation is dependent on the incident energy. A similar feature is seen in

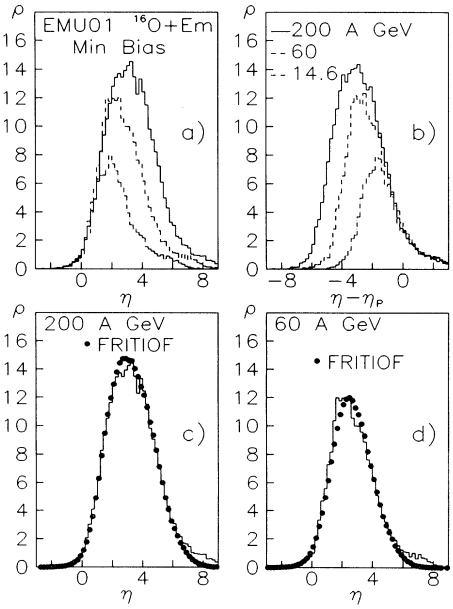

FIG. 1. Pseudorapidity distributions of charged particles in oxygen-induced interactions with emulsion at 14.6, 60, and 200 GeV/nucleon for the minimum-bias samples. (a) In the target rest frame. (b) In the projectile rest frame. (c) Comparison between data and the FRITIOF model at 200A GeV. (d) Comparison between data and the FRITIOF model at 60A GeV.

Fig. 1(b) where the three energies show limiting fragmentation also in the projectile region for $\eta - \eta_p \geq -1$. Again an energy dependence of the size of the region is seen. It is interesting to observe that at 14.6A GeV the shape of the distribution is quite dominated by the large-η tail, but still this tail is identical to the tails observed at higher energies. It is important to note that the exclusion of interactions due to electromagnetic dissociation and elastic scattering is essentially for obtaining these results.

In Figs. 1(c) and 1(d) the pseudorapidity distributions from 200A and 60A GeV are compared to the corresponding distributions from the FRITIOF samples. It is essential to point out that no normalization is involved in this figure; i.e., the average multiplicities obtained by FRITIOF are in excellent agreement with the data as can be seen in Table I. The comparison of the distributions reveals a very nice agreement except for the region $\eta \geq \eta_p$, where the fragmentation of the spectator parts of the projectiles become important. The fragmentation products from these parts are, however, not included in the distributions from the FRITIOF model.

In order to obtain a sample of central events, the N_h information is normally used in emulsion experiments. It has been observed in hadron-induced interactions that the N_h distribution is energy dependent over a large range of energies. Furthermore, N_h was found to be strongly correlated to the centrality of the event.[4] The same has been conjectured to be true also when heavy ions are used as projectiles. When comparing data with models like FRITIOF, N_h cuts are, however, not a good criterion for centrality, since the target breakup is, up to the present date, not included in these models. We therefore introduce the forward charge flow Q_{ZD}, defined as $Q_{ZD} = \sum Z_{\text{frag}} + n(\eta \geq \eta_{ZD})$, where Z_{frag} is the charge of an observed projectile fragment with $Z \geq 2$, and $n(\eta \geq \eta_{ZD})$ is the number of shower particles with $\eta \geq \eta_{ZD}$, given by $\eta_{ZD} = \eta_p + 0.36$. Because of the limiting fragmentation seen in Fig. 1, Q_{ZD} is expected to be an energy-independent quantity in the energy range studied. The value of η_{ZD} is chosen as a compromise between not having too many produced pions inside the cone and not having too many spectator protons outside. Thus Q_{ZD} is analogous to the forward energy flow E_{ZD}, used by some of the current counter experiments.[1] The corresponding angles Θ_{ZD} are 39, 10, and 3 mrad for 14.6, 60, and 200 GeV/nucleon, respectively.

In Fig. 2 we compare two different central samples from 200A GeV, both consisting of about 11% of the minimum-bias sample, one with $N_h \geq 23$ and one with $Q_{ZD} \leq 2$. We observe a similarity between the two samples and conclude that the two cuts are comparable as criteria for centrality. It is interesting to observe that the information obtained either from the projectile or from the target fragmentation regions can be used to deduce the particle density in the central region. We observe, however, a small indication that Q_{ZD} might be somewhat more efficient, since the density of observed particles is (10–20)% higher in the region $2 \leq \eta \leq 4$ using that quantity.

For the FRITIOF model, Q_{ZD} can be calculated as the sum of the number of projectile spectator protons and the number of particles observed in the cone $\Theta \leq \Theta_{ZD}$, and in Fig. 3 we compare how the 200A-GeV events fall in the Q_{ZD}-n_s space, for the data and for the FRITIOF model, respectively. The two plots show great similarities, with the bulk of the distributions with Q_{ZD} around 7 and 8. The width of the n_s distribution for a given Q_{ZD} value is well described by the model.

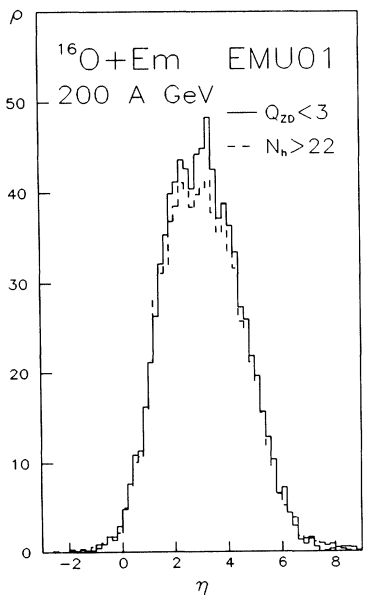

FIG. 2. Pseudorapidity distributions of charged particles in oxygen-induced interactions with emulsion at 200A GeV for two different central samples.

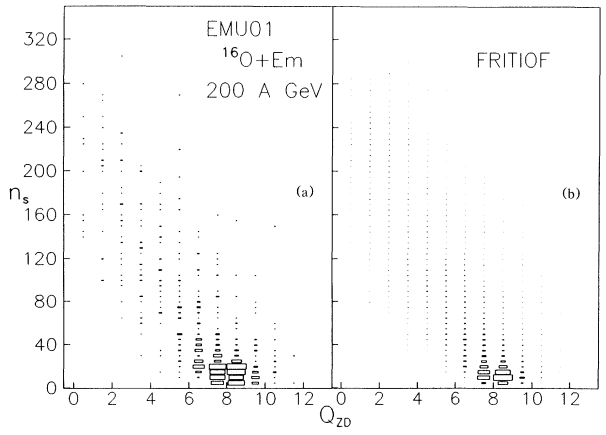

FIG. 3. The event distribution in Q_{ZD}-n_s space for (a) the 200A-GeV data and (b) the corresponding FRITIOF sample.

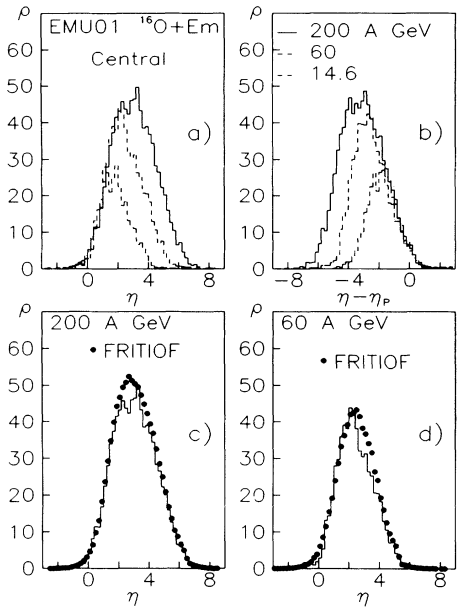

FIG. 4. As for Fig. 1, but for central $^{16}O+Ag(Br)$ samples with $Q_{ZD} \leq 2$.

For the data samples we now introduce the cut $Q_{ZD} \leq 2$ combined with $N_h \geq 10$, the last cut being implemented in order to get rid of the small fraction of central interactions from the light component (CNO) in the emulsions, leaving a clean sample of central events having interacted with Ag or Br. The $N_h \geq 10$ cut removes between (5–10)% of the events remaining after the first cut has been applied. The same restriction was implemented on the FRITIOF events by requiring $Q_{ZD} \leq 2$. The FRITIOF model does not include any target cascade and is thus not able to reproduce the N_h production, and therefore only interactions with bromine or a heavier target were considered. The percentage of the events from the different samples fulfilling the centrality criterion is given in Table I together with their statistical errors. As can be seen in the table, the experimental event fractions seem to be independent of energy within the statistical errors. The apparent increase with increasing energy might be interpreted as a sign of a decreasing transparency with increasing energy, for the most central events, but this effect is hardly statistically significant. In the model, however, a similar statistically significant effect is present. In the model this means that the produced strings, covering a larger and larger region of phase space as the incident energy increases, encounter an increasing difficulty to stretch out all the way into the projectile fragmentation region, giving particles a slight shift to larger angles. This is a small effect and is evidently not visible in the limiting fragmentation behavior. Furthermore, the fractions are somewhat larger in the data than in the model, indicating a larger stopping power than predicted by the picture of independently fragmenting strings. Note that the stopping power defined as the energy missing in a forward cone does not necessarily have the same energy dependence as a similar quantity related to, for instance, the transverse-energy production in the central region.

In Fig. we show the pseudorapidity distributions obtained for the central samples in the same kind of representation as in Fig. 1. We observe a similar limiting fragmentation behavior as before for the minimum-bias sample, although the shapes of the individual spectra have changed. In the comparisons with FRITIOF we see that the model somewhat overestimates the average multiplicities in the region $2 \leq \eta \leq 4$, and the peak value at $60A$ GeV seems to be shifted to a larger value of η. The overall behavior is, however, in quite good agreement with the data.

To conclude, we note that limiting fragmentation concerning heavy-ion collisions is fulfilled in the energy range 14.6–200 GeV/nucleon for both the target and the projectile fragmentation regions, independent of the centrality of the interactions. The forward charge flow seems to be a convenient measure of centrality, well suited for model comparisons.

We express our thanks to the CERN staff of the Proton Synchrotron and Super Proton Synchrotron for their outstanding performance in producing the ^{16}O and ^{32}S beams for the experiment, with special thanks to G. Vanderhaeghe, K. Ratz, N. Doble, P. Grafström, M. Reinharz, H. Sletten, and J. Wotschack and also to D. Beavis, who helped with the exposures at BNL. We are also extremely thankful for the contributions given by the scanning and measuring staffs within the collaboration. The financial support from the Swedish Natural Science Research Council (NFR), the German Federal Minister of Research and Technology, the Department of University Grants Commission, Government of India, the National Natural Science Foundation of China, and the U.S. Department of Energy and NSF are gratefully acknowledged.

[1]*Quark Matter 1987, Proceedings of the Sixth International Conference on Ultra-Relativistic Nucleus-Nucleus Collisions, Nordkirchen, Federal Republic of Germay, 24–28 August 1987* [Z. Phys. C **38** (1988)]; WA80 Collaboration, R. Albrecht *et al.*, Phys. Lett. B **202**, 596 (1988); NA35 Collaboration, H. Ströbele *et al.*, Z. Phys. C **38**, 89 (1988); E802 Collaboration, M. Tannenbaum *et al.*, in Proceedings of the Third International Conference on Nucleus-Nucleus Collisions, Saint Malo, France, June 1988 (to be published); EMU07 Collaboration, L. M. Barbier *et al.*, Phys. Rev. Lett. **60**, 405 (1988); EMU08 Collaboration, P. L. Jain *et al.*, Phys. Rev. Lett. **59**, 2531 (1987).

[2]EMU01 Collaboration, M. I. Adamovich *et al.*, Phys. Lett. B **201**, 397 (1988); EMU01 Collaboration, S. Garpman *et al.*, Nucl. Instru. Methods Phys. Res., Sect. A **269**, 134 (1988).

[3]B. Nilsson-Amqvist and E. Stenlund, Comput. Phys. Commun. **43**, 387 (1987).

[4]E. Stenlund and I. Otterlund, Nucl. Phys. **B198**, 407 (1982).